BEST AVAILABLE IMAGES

Defective images within this document are accurate representations of the original documents submitted by the applicant.

Defects in the images may include (but are not limited to):

- BLACK BORDERS
- TEXT CUT OFF AT TOP, BOTTOM OR SIDES
- FADED TEXT
- ILLEGIBLE TEXT
- SKEWED/SLANTED IMAGES
- COLORED PHOTOS
- BLACK OR VERY BLACK AND WHITE DARK PHOTOS
- GRAY SCALE DOCUMENTS

IMAGES ARE BEST AVAILABLE COPY.

As rescanning documents *will not* correct images, please do not report the images to the Image Problem Mailbox.

A cardiac myocyte vascular endothelial growth factor paracrine pathway is required to maintain cardiac function

Frank J. Giordano*†‡, Hans-Peter Gerber†§, Simon-Peter Williams§, Nicholas VanBruggen§, Stuart Bunting§, Pilar Ruiz-Lozano¶, Yusu Gu¶, Anjali K. Nath*, Yan Huang*, Reed Hickey*, Nancy Dalton¶, Kirk L. Peterson¶, John Ross, Jr.¶, Kenneth R. Chien¶, and Napoleone Ferrara§

*Cardiovascular Gene Therapy Program, Department of Medicine, Yale University School of Medicine, Boyer Center for Molecular Medicine, 295 Congress Avenue, Room 336C, New Haven, CT 06520; §Genentech, Inc., 1 DNA Way, South San Francisco, CA 94080-4990; and ¶University of California at San Diego–Salk Program in Molecular Medicine, University of California at San Diego School of Medicine, 9500 Gilman Drive, La Jolla, CA 92037

Edited by Sherman M. Weissman, Yale University School of Medicine, New Haven, CT, and approved February 20, 2001 (received for review August 28, 2000)

The r le of the cardiac myocyte as a mediator of paracrine signaling in the heart has remained unclear. To address this issue, we generated mice with cardiac myocyte-specific deletion of the vascular endothelial growth factor gene, thereby producing a cardiomyocyte-specific knockout of a secreted factor. The hearts of these mice had fewer coronary microvessels, thinned ventricular walls, depressed basal contractile function, induction of hypoxia-responsive genes involved in energy metabolism, and an abnormal response to β-adrenergic stimulation. These findings establish the critical importance of cardiac myocyte-derived vascular endothelial growth factor in cardiac morphogenesis and determination of heart function. Further, they establish an adult murine model of hypovascular nonnecrotic cardiac contractile dysfunction.

Factors secreted by nonmuscle cells can have significant paracrine effects on cardiac myocytes (1–3). The critical importance of these effects on cardiac muscle is illustrated by the recent finding of stress-induced heart failure and cell death in mice lacking the gp130 cytokine signaling pathway in the myocardium (4). Although the significance of paracrine signaling from nonmyocytes to myocytes in the heart now is established firmly, the relative importance of cardiomyocyte-derived factors as paracrine or autocrine effectors in the heart has remained unclear. Cardiac myocytes constitute two-thirds of total heart volume, thus secretion of factors from this cell population may be of considerable importance (5, 6). Moreover, alterations in cardiomyocyte-derived paracrine or autocrine signals, such as may occur in progressive heart failure or with myocyte loss secondary to myocardial infarction, may have important clinical repercussions. Cardiomyocyte-derived transforming growth factor (TGF)-β1 and metalloproteinases, for example, could have marked effects on ventricular remodeling after myocardial injury (7, 8). Production of tumor necrosis factor (TNF)-α by cardiomyocytes can lead to cardiac pump failure with progressive fibrosis and cardiomyocyte apoptosis (9). Cardiomyocyte-derived factors may also play critical roles in the development, growth, and maintenance of the coronary vasculature.

Using Cre-lox technology, we investigated the role of cardiac myocyte secretory function by generating mice with cardiomyocyte-specific deletion of exon 3 in the gene encoding vascular endothelial growth factor A (VEGF-A) (10, 11). This deletion results in the loss of all VEGF-A isoforms. These mice have reduced body weights and their hearts are thin-walled, dilated, hypovascular, and display definitive basal contractile dysfunction. Furthermore, there is induction of hypoxia-responsive genes in the knockout (KO) hearts without evidence of myocardial necrosis or replacement fibrosis. Thus, we establish a critical role for the cardiac myocyte as a secretory cell, and determine that cardiac muscle is the major source of VEGF in the heart. Further, we demonstrate that a single gene defect in the heart can have significant effects on whole-body growth. Finally, we describe the first adult murine model to our knowledge of coronary hypovascularization with chronic nonnecrotic contractile dysfunction. This model may prove valuable in the study of protein and gene therapy-based strategies to stimulate cardiac angiogenesis therapeutically. It also may prove valuable in the study of the molecular mechanisms underlying myocardial contractile dysfunction associated with chronic recurrent ischemia as occurs in patients with advanced coronary artery disease (12).

Methods

Generation and Characterization of Conditional KO Mice. "Floxing" of VEGF exon 3 was performed in embryonic stem cells by using a double-selection VEGF targeting vector (Fig. 1*A*) (10). Resulting VEGF-LoxP mice were bred with knockin mice carrying the Cre-recombinase gene under control of the endogenous MLC2v promoter; directing Cre expression and consequent VEGF gene deletion to ventricular cardiac myocytes (4, 13). The offspring were genotyped as described (4, 10). Cardiac myocytes and nonmyocytes were isolated from KO and control hearts by collagenase digestion as described (4). VEGF gene deletion was documented by Southern blot analysis of *Eco*RI-digested genomic DNA from these cells by using a probe specific for the exon 1 region.

***In Vivo* Characterization of Cardiac Function.** MRI was performed at 4.7 T in a 3-cm quadrature volume coil. Mice were anesthetized with 1–1.5% isoflurane in 70/30 nitrous oxide/oxygen mixture with body temperature held at 36–37°C. Cine-FLASH imaging was used with 9–15 cine images per cycle; delay between frames was 11 ms. A scout long-axis view was used to guide short- axis imaging. Seven 1.0-mm short-axis slices covered the entire left ventricle. Echocardiography and hemodynamic assessment were performed as described (14, 15). Mice were age-matched for all functional studies.

Analysis of Gene Expression. Expression of VEGFs A–C, placental growth factor, VEGF receptors Flk-1, Flt-1, and Flt-4, and additional genes with reported roles in angiogenesis, vascular remodeling, or the cellular hypoxic response, was quantitated at

This paper was submitted directly (Track II) to the PNAS office.

Abbreviations: VEGF, vascular endothelial growth factor; KO, knockout; cmVEGF-null, cardiomyocyte-specific VEGF KO; RT-PCR, reverse transcription–PCR; PECAM, platelet–endothelial cell adhesion molecule; E*n*, embryonic day *n*; LDH, lactate dehydrogenase; Glut-1, glucose transporter 1.

†F.J.G. and H.-P.G. contributed equally to this work.

‡To whom reprint requests should be addressed. E-mail: Frank.Giordano@yale.edu.

The publication costs of this article were defrayed in part by page charge payment. This article must therefore be hereby marked "*advertisement*" in accordance with 18 U.S.C. §1734 solely to indicate this fact.

www.pnas.org/cgi/doi/10.1073/pnas.091415198

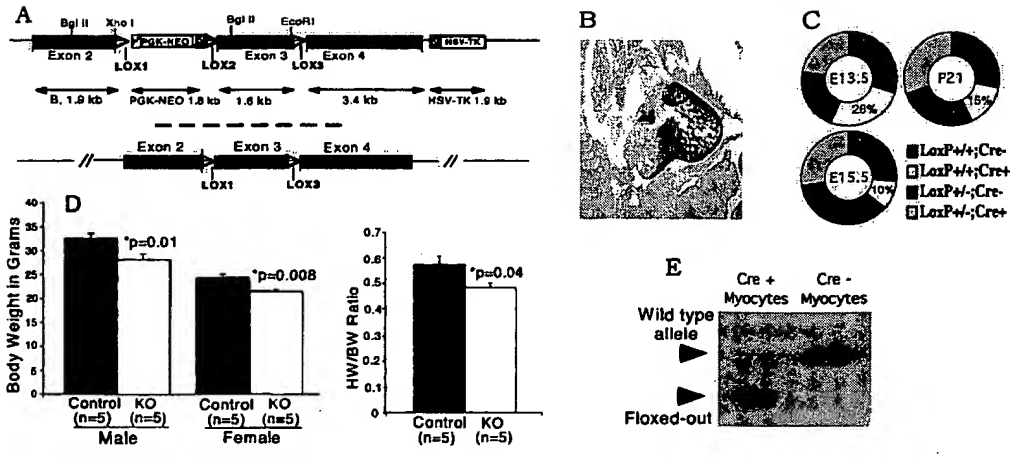

Fig. 1. Cardiac myocyte-specific VEGF gene targeting. (*A*) VEGF-LoxP targeting vector (*Upper*) and resulting genomic allele after Cre-recombinase-mediated deletion of the neo cassette (*Lower*). Excision of exon 3 results in deletion of all known VEGF-A isoforms. (*B*) *In situ* hybridization in E13.5 embryo demonstrating the restriction of MLC2v gene expression to ventricular cardiac myocytes. (*C*) Genotype frequencies from timed matings (on E13.5 and E15.5 of embryonic development, and postnatal day 21). Expected representation of $Cre^+/VEGF\text{-}LoxP^{+/+}$ is 25% in all cases. (*D*) Body weight (*Left*) and heart weight/body weight ratios (HW/BW; *Right*) at 3 months. (*E*) Southern blot analysis of *Eco*RI-digested genomic DNA obtained from cardiac myocytes prepared by collagenase digestion of $VEGF\text{-}LoxP^{+/+} \times Cre^+$ and $VEGF\text{-}LoxP^{+/+} \times Cre^-$ hearts. First lane, high-efficiency floxing out of VEGF exon 3 in $VEGF\text{-}LoxP^{+/+} \times Cre^+$ cardiac myocytes resulting in a smaller *Eco*RI genomic fragment (lower band); second lane, intact VEGF-A *Eco*RI genomic fragment (upper band) in control ($VEGF\text{-}LoxP^{+/+} \times Cre^-$) cardiac myocytes.

the mRNA level by using real-time reverse transcription–PCR (RT-PCR) analysis (16). RNA was isolated from frozen hearts of five control ($VEGF\text{-}Lox^{+/+}$, Cre^-) and five test mice ($VEGF\text{-}Lox^{+/+}$, Cre^+) by using the Stat 60 method (Tel-Test, Friendswood, TX), and was purified on RNeasy quick-spin columns (Qiagen, Chatsworth, CA). Per reaction, 100 ng of total RNA was analyzed by using the RT-PCR kit from Perkin–Elmer following the manufacturer's instructions. Reactions were run in 96-well plates in a model 7700 sequence detector (Applied Biosystems) and results were analyzed by using SEQUENCE DETECTION software (Applied Biosystems). RT-PCR conditions were 30 min at 48°C, 10 min at 95°C, and 40 cycles of 30 s at 95°C and 90 s at 60°C. Relative RNA equivalents for each sample were obtained by standardizing to glyceraldehyde-3-phosphate dehydrogenase (GAPDH) levels. Each of the five samples per group was run in duplicates and the average relative RNA equivalents per sample pair was used for further analysis. Statistical analysis was performed by using ANOVA software (Abacus Concepts, Berkeley, CA). VEGF protein levels were evaluated in protein homogenates from control and cardiomyocyte-specific VEGF KO (cmVEGF-null) hearts by a sensitive ELISA method (Quantikine Immunoassay R&D Systems, Minneapolis).

Immunohistochemistry, *in Vivo* Platelet–Endothelial Cell Adhesion Molecule (PECAM) Binding, *in Situ* Hybridization, Histology, and Morphometrics. For histology, tissue was fixed in 4% paraformaldehyde and paraffin-embedded. Sections were stained with hematoxylin and eosin, Gill's stain, or trichrome. For immunohistochemistry, paraffin-embedded and frozen sections were used. VEGF immunostaining was performed with a monoclonal anti-VEGF-A antibody (R & D Systems). PECAM immunostaining was performed on acetone-fixed sections by using a rat anti-mouse monoclonal antibody (PharMingen). Capillary counts were obtained by counting 10 separate high-power fields per section and comparing counts to the number of nuclei in the same fields. For *in vivo* PECAM binding studies, a validated method was used (17). Briefly, a monoclonal antibody against PECAM-1 was radiolabeled with ^{125}I and administered systemically to control and cmVEGF-null mice via tail-vein injection. Labeled antibody was allowed to circulate and bind for 30 min. Mice were then killed and tissue was collected for well counting and protein quantitation. *In situ* hybridization was performed on paraffin-embedded sections by using an ^{35}S-labeled probe for mouse MLC2v. Microfil polymer casts (Flow Tech, Carver, MA) of the coronary vasculature were made by retrograde aortic perfusion at constant pressure on a modified Langendorf apparatus after maximal vasodilation with intravascular nitroglycerin.

Results

Generation of cmVEGF-Null Mice. By using double- selection gene targeting in embryonic stem cells, we created mice with LoxP sites inserted into intron sequences flanking exon 3 of the VEGF-A gene (Fig. 1*A*) (10). In a previous study, targeting of this exon to achieve a global KO resulted in efficient VEGF-A gene deletion without production of a secreted dominant-negative truncation peptide (18). Cardiac myocyte-specific VEGF gene deletion was accomplished by mating VEGF-loxP mice with myosin light chain 2v (MLC2v)-Cre mice that direct Cre expression specifically to ventricular cardiomyocytes (Fig. 1*B*) (4, 13). Genotype analysis of offspring revealed viable homozygous cmVEGF-null mice, but at a 40% lower than expected gene frequency. This finding demonstrated that selective deletion of the VEGF-A gene from cardiac myocytes could cause variable embryonic lethality. Timed matings revealed expected genotype ratios at embryonic day (E)12.5 but significant embryonic lethality was apparent by E15.5 (Fig. 1*C*). Liveborn cmVEGF-null mice appeared healthy with normal postnatal survival into adulthood but had lower body weights than control litter mates: females, 21.5 ± 0.270 vs. 24.2 ± 0.675 g, $P = 0.008$, $n = 5$; males, 28.0 ± 1.3 vs. 32.6 ± 0.952 g, $P = 0.01$, $n = 5$. Adult heart weight/body weight ratios also were reduced in the KOs: 0.482 ± 0.021 vs. 0.574 ± 0.033 g, $P = 0.04$, $n = 5$ (Fig. 1*D*). cmVEGF gene deletion was documented by Southern blot analysis of cardiac myocyte DNA extracted from control and cmVEGF-null hearts (Fig. 1*E*). Nonmyocyte DNA from the KO mice demonstrated no evidence of gene deletion, whereas cardiomyocyte DNA consistently demonstrated ≈85–90% efficiency deletion of VEGF exon 3. These data establish the efficiency of MLC2v-Cre-directed VEGF deletion specifically in cardiomyocytes, and are consistent with previous work establishing cardiomyocyte-specific excision of LoxP-flanked genes by MLC2v-Cre (4).

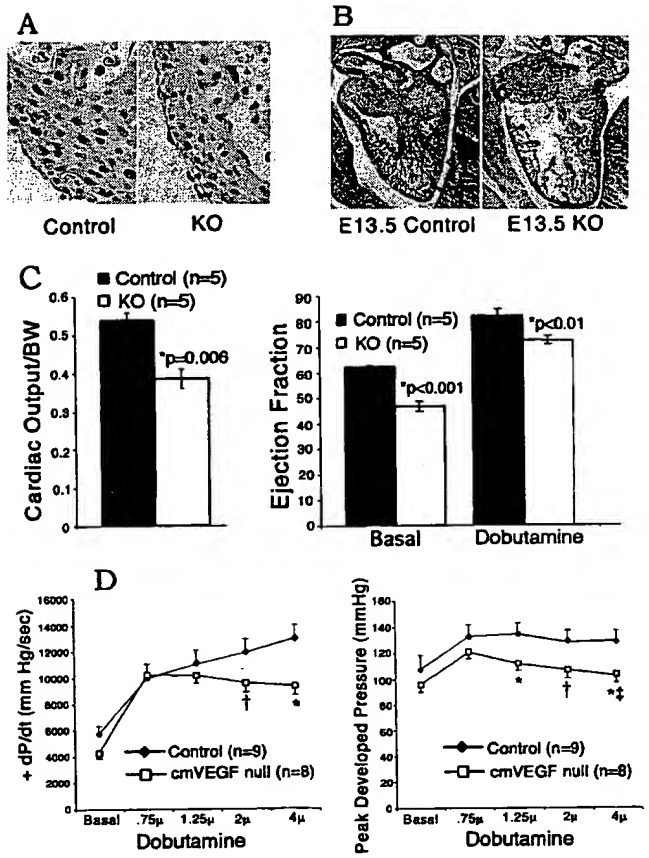

Fig. 2. Morphometry and function of cmVEGF-null hearts. (*A*) Hematoxylin and eosin staining of E13.5 myocardium from cmVEGF-null (*Right*) and control (*Left*) hearts demonstrating no differences in myocyte organization and morphometry. (*B*) Ventricular thinning in cmVEGF-null mice. Whole mount sections of control (*Left*) and cmVEGF-null (*Right*) hearts obtained from E13.5 embryos. (*C*) Magnetic resonance determination of heart function. Cardiac output per body weight (BW) (left) and percent ejection fraction under basal conditions and with β-adrenergic stimulation (dobutamine) (right). (*D*) Hemodynamic responses to β-adrenergic stimulation with graduated doses of dobutamine. Rate of rise of left ventricular pressure during systole ($+dP/dt$ in mmHg/sec; *, $P = 0.01$ and †, $P = 0.09$) (*Left*). Peak developed left ventricular pressure in mmHg (*, $P < 0.05$; †, $P = 0.07$; and ‡, $P < 0.001$ relative to peak pressure at 0.75-μg dobutamine dose) (*Right*).

Ventricular Thinning, Dilation, and Diminished Contractile Function in cmVEGF-Null Hearts. Embryos were dissected after timed matings to investigate the morphology of cmVEGF-null hearts before embryonic lethality and resorption. Histologic examination of sections from E13.5 embryos revealed no differences in myocyte size or shape and no basic alterations in myocardial architecture (Fig. 2*A*). At E13.5, analysis of Gill's stained sections revealed thinning of the ventricular wall in cmVEGF-null hearts as compared with control embryos from the same gestation (Fig. 2*B*). This finding was variable at this gestational age, and was investigated further in age-matched adult mice by using two-dimensional and M-mode echocardiography, which revealed significant diastolic and systolic thinning of the septum and posterior free wall of the left ventricle in cmVEGF-null hearts (Table 1). These data remained highly significant when adjusted for heart size by using the ventricular end-diastolic diameter as a reference. Echocardiograms also revealed significant dilation of cmVEGF-null hearts relative to body weight. Thus, cardiac myocyte-specific deletion of VEGF results in a dilated thin-walled adult heart. Although this morphometric phenotype is consistent with that of an ischemic cardiomyopathy, histologic

Table 1. Echocardiographic analysis of cardiac morphometry and function

Measurement	cmVEGF-null ($n = 8$)	Control ($n = 10$)
LVEDD/BW	0.16 ± 0.02*	0.13 ± 0.02
SEPth, mm	0.61 ± 0.09*	0.75 ± 0.11
PWth, mm	0.86 ± 0.17*	1.07 ± 0.16
SEPth/EDD	0.16 ± 0.03*	0.19 ± 0.02
PWth/EDD	0.15 ± 0.03*	0.19 ± 0.02
FS, %	22.4 ± 5.1†	30.8 ± 4.7
Mean Vcf, circ/sec	4.01 ± 0.95‡	5.31 ± 1.14
HR, beat/min	383 ± 72	406 ± 66

LVEDD, left ventricular end-diastolic dimension; BW, body weight; SEPth, septal-wall thickness; PWth, posterior-wall thickness; mean Vcf, mean velocity of circumferential fiber shortening in circumference per sec; FS, percent fractional shortening calculated as [(LVEDD − LV end systolic dimension)/LVEDD] × 100; HR, heart rate. *, $P = 0.01$, †, $P < 0.005$, ‡, $P = 0.02$.

examination revealed no evidence of cardiomyocyte necrosis or myocardial fibrosis. Morphometric analysis of the adult heart did not reveal valve lesions, evidence of anatomic shunts, or any differences in cardiac trabeculations. Terminal deoxynucleotidyltransferase-mediated dUTP end labeling (TUNEL) staining was negative, indicating no evidence of ongoing apoptosis in the thinned myocardium but not precluding the possible contribution of an apoptotic mechanism in the pathogenesis of ventricular thinning (data not shown).

The effects of cardiomyocyte VEGF gene deletion on contractile function were assessed by echocardiography, MRI, and high-fidelity catheter-based hemodynamic evaluation. Baseline echocardiography performed on unstressed hearts revealed significant reductions of percent fractional shortening and the velocity of circumferential shortening in cmVEGF-null mice (Table 1). MRI demonstrated a reduced ejection fraction: 46.8 ± 1.8% vs. 62.3 ± 0.3%; $P < 0.001$ and low cardiac output/body weight: 0.385 ± 0.025 vs. 0.537 ± 0.019; $P = 0.006$ in cmVEGF-null hearts ($n = 5$ for all groups), providing clear documentation of basal cardiac pump dysfunction. β-Adrenergic stimulation with dobutamine improved ejection fraction in both KO and control hearts, but the relative reduction in cmVEGF-null hearts remained significant: 72.4 ± 1.5 vs. 82.0 ± 2.6%, $P < 0.01$, $n = 5$ (Fig. 2*C*). Catheter-based hemodynamic assessment at baseline and with increasing doses of dobutamine demonstrated a significant reduction of graduated contractile response in cmVEGF-null hearts. At higher levels of β-adrenergic stimulation, the rate of rise of left ventricular pressure during systole ($+dP/dt$) was reduced relative to controls, and demonstrated a plateau beyond which increasing the dose of dobutamine had no positive effect on contractility. cmVEGF-null mice also demonstrated a significant fall in peak developed blood pressure at higher dobutamine doses (Fig. 2*D*). These changes are not attributable to the MLC2v-Cre background, as extensive previous assessment of MLC2v-Cre mice revealed no basal or inducible abnormalities in cardiac morphometry or function as a consequence of the Cre cassette (13). Also, assessment of cmVEGF heterozygous KOs revealed no significant differences in morphometry or function relative to controls (data not shown).

Global Reduction in VEGF-A and Vascularity in cmVEGF-Null Hearts. To assess the impact of cardiomyocyte-specific VEGF gene deletion on total VEGF levels in the heart, real-time quantitative RT-PCR was performed on RNA extracted from whole hearts. Remarkably, there was a 6-fold reduction of VEGF mRNA in the cmVEGF-null hearts, indicating that cardiac myocytes are the major source of VEGF in the heart: 0.28 ± 0.08 vs. 1.71 ± 0.13 relative units; $P = 0.004$; $n = 5$ per group (Fig. 3*A*). VEGF

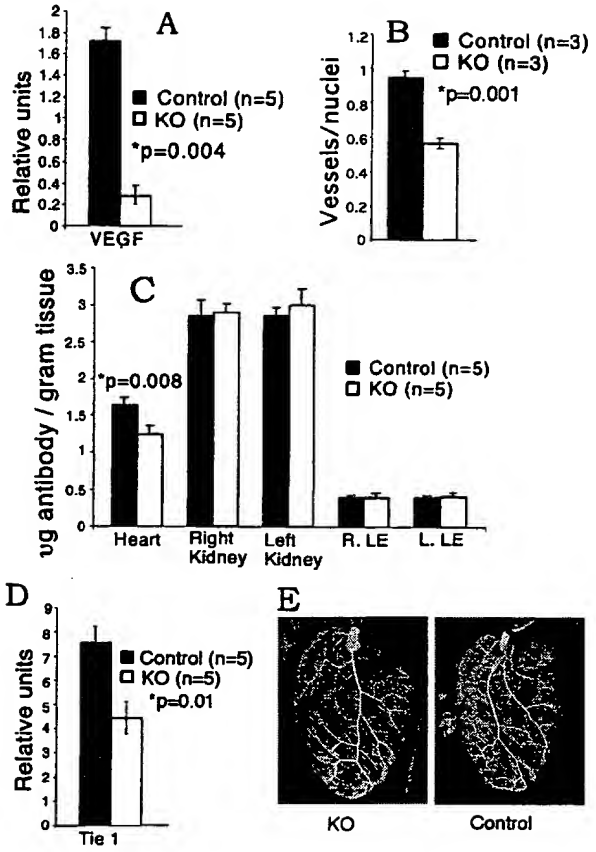

Fig. 3. VEGF expression, vascularization, and hypoxic gene induction in cmVEGF-null hearts. (*A*) Quantitative real-time RT-PCR determination of VEGF mRNA (relative units). (*B*) PECAM-stained microvessels/myocyte nuclei (average count, 10 high-power fields per section). (*C*) *In vivo* ^{125}I-labeled anti-PECAM antibody binding (expressed as μg of antibody per g of tissue). (*D*) Quantitative RT-PCR of cardiac mRNA for Tie-1 (relative units). (*E*) Polymer cast of coronary vasculature demonstrating normal macrovessel morphometry.

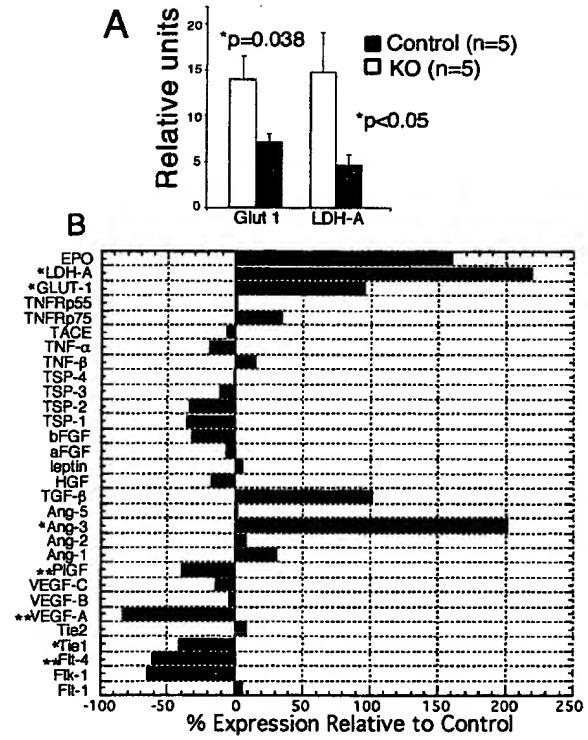

Fig. 4. Induction of hypoxia-responsive genes and alterations of gene-expression profile in cmVEGF-null hearts. (*A*) Increased expression of hypoxia-responsive genes, Glut-1 and LDH-A, in cmVEGF-null hearts (quantitative RT-PCR expressed in relative units). (*B*) Relative mRNA levels in cmVEGF-null hearts expressed as percent change from control (% change = [(cmVEGF − control)/control]·100; $n = 5$ for both groups). EPO, erythropoietin; TNF, tumor necrosis factor; TNFRp55–p75, TNF receptors; TSP1–4, thrombospondins; TACE, tumor necrosis factor α convertase; Ang-1–5, angiopoietins); HGF, hepatocyte growth factor; Tie-1, Tie-2, Flk1, Flt1, and Flt4, vascular tyrosine kinase receptors. *, $P < 0.05$; **, $P < 0.005$.

protein expression was undetectable by a sensitive ELISA method in the cmVEGF-null hearts, as compared with 11.25 ± 3.37 pg/mg tissue in the wild-type hearts. Immunostaining with an anti-VEGF antibody demonstrated diffuse staining in control myocardium. There was a markedly reduced intensity of VEGF immunostaining in the myocardium of cmVEGF-null hearts that was generally homogeneous, with occasional areas of increased immunoreactivity (not shown).

To determine the effects of cardiomyocyte-specific VEGF deletion on cardiac vascularization, we performed PECAM immunohistochemistry and RT-PCR for endothelial cell markers, and measured *in vivo* radiolabeled PECAM binding. Capillary density was significantly diminished in cmVEGF-null hearts, as was the capillary to myocyte nuclei ratio: 0.56 ± 0.03 vs. 0.94 ± 0.04; $P = 0.001$; $n = 4$ per group; 10 high-powered fields per section (Fig. 3*B*). Corroborative studies demonstrated reduced *in vivo* binding of radiolabeled anti-PECAM antibody in cmVEGF-null hearts: 1.245 ± 0.119 vs. 1.646 ± 0.104 μg of antibody per g of tissue; $P = 0.003$; $n = 5$. Conversely, no reductions in antibody binding were seen on analysis of tissue from kidney or upper and lower extremities (Fig. 3*C*). Consistent with the PECAM data, RT-PCR demonstrated a reduction in Tie-1 mRNA in cmVEGF-null hearts indicative of a generalized reduction in endothelial cells: 4.4 ± 0.65 vs. 7.5 ± 0.7 relative units; $P = 0.01$; $n = 5$ (Fig. 3*D*). Immunostaining for smooth muscle cell α-actin did not reveal perceptible differences in the number of larger coronary vessels (data not shown). To investigate the effects of cardiomyocyte VEGF deletion on general coronary artery patterning and large-vessel distribution, hearts from control and cmVEGF-null mice were perfused with a synthetic polymer to create vascular casts that were then analyzed with high-resolution stereomicroscopy. Although there were natural variations in coronary anatomy among all of the animals, there were no consistent differences in branching or patterning of larger coronary vessels correlating with genotype (Fig. 3*E*). Cardiac myocyte-restricted deletion of the VEGF-A gene thus leads to a marked reduction in heart VEGF expression, resulting in a significantly diminished coronary microvasculature with preservation of the coronary macrovasculature.

Altered Gene-Expression Profile in cmVEGF-Null Hearts. Despite the absence of apparent cardiomyocyte necrosis or cardiac fibrosis, cmVEGF-null hearts exhibit significant baseline contractile dysfunction. Given the relative hypovascularity of these hearts, this dysfunction could reasonably be attributed to myocardial ischemia. To address this possibility, we analyzed the expression of representative ischemia-responsive genes in KO and control hearts. The promoters for Glut-1 and lactate dehydrogenase A (LDH-A) contain a hypoxia response element that binds the hypoxia-inducible factor (HIF)-1α, resulting in transcriptional up-regulation (19, 20). Quantitative RT-PCR revealed significantly increased expression of the Glut-1 glucose transporter and the glycolytic enzyme LDH-A in cmVEGF-null hearts, consistent with a switch in myocardial energy metabolism: Glut-1, 13.90 ± 2.61 vs. 7.11 ± 0.847 relative units, $P = 0.038$; LDH-A,

14.72 ± 4.38 vs. 4.61 ± 1.13 relative units, $P = 0.047$ (Fig. 4*A*). These data support a role for ischemia in the basal left ventricular pump dysfunction noted in the KO hearts.

To further define the effects of cardiomyocyte-specific VEGF-A deletion on gene-expression profiles in the heart, relative expression levels of genes with purported roles in angiogenesis, vascular remodeling, or the cellular hypoxic response were determined by quantitative RT-PCR. Interestingly, there were no compensatory increases in mRNA levels for VEGF-B and -C, and there was a significant reduction in the relative expression of placental growth factor (40% decrease from basal; $P < 0.005$). There was a significant increase in angiopoietin 3 (200% increase; $P < 0.05$), and an increase in transforming growth factor $\beta 1$ that trended toward but did not reach significance. VEGF-C receptor Flt-4 was reduced (60% decrease; $P < 0.05$), and there was a 65% reduction in VEGF receptor Flk-1 that did not reach significance ($P = 0.12$). VEGF receptor Flt-1 was not reduced in cmVEGF-null hearts nor was the Tie-2 tyrosine kinase receptor, both of which contain hypoxia response elements in their promoters. Results for these and additional relevant genes are shown graphically (Fig. 4*B*).

Discussion

In these studies, we describe to our knowledge the first cardiac-specific KO of a secreted factor, and reveal a critical role of the cardiac myocyte as a secretory cell and paracrine effector. Specifically, we establish a crucial requirement for cardiac myocyte-derived VEGF in development of the coronary microvasculature and document that developmental deletion of cardiac myocyte VEGF results in contractile dysfunction of the adult heart. Cardiac myocytes represent less than one-third of the total cell number in the heart, yet we demonstrate a 6-fold reduction of VEGF expression in cmVEGF-null hearts. This finding indicates that nonmyocytes, although present in greater number, cannot fully compensate for the loss of cardiomyocyte-derived VEGF. This dependence on cardiac myocyte secretory function may have significant clinical implications. It is conceivable that loss of cardiac myocytes caused by infarction or other causes may significantly alter myocardial paracrine signaling and have effects beyond those attributable purely to the loss of contractile elements. Despite acute induction of VEGF expression in the periinfarct zone, chronic regional reductions in cardiomyocyte-derived VEGF (or other growth factors) might negatively influence postinfarction ventricular remodeling or contribute to the pathophysiology of progressive ischemic myocardial dysfunction (21). This is an important consideration that may support an expanded role for the use of growth factors therapeutically in ischemic heart disease.

Stimulated therapeutic angiogenesis to treat ischemic heart disease has been shown to be feasible in animal studies and is being tested in clinical trials (22–24). A variety of diverse approaches for delivering angiogenic genes or proteins to the heart are being investigated. The data we present here demonstrate the importance of local angiogenic factor concentration as a determinant of angiogenic effect, and lend support to strategies predicated on local delivery of angiogenic proteins or genes to the myocardium. Such considerations could have significant implications regarding the route of therapeutic administration of angiogenic factors.

cmVEGF-null hearts have diminished contractile function at rest. The etiology of this basal contractile dysfunction is not entirely clear. One explanation is ischemic myocardial dysfunction based on hypoperfusion. We have shown that cmVEGF-null hearts are hypovascular at the microvessel level and exhibit basal induction of the hypoxia-responsive genes Glut-1 and LDH-A. The VEGF receptor Flt-1 and the Tie-2 receptor are inducible by hypoxia. Expression of these receptors is not decreased in cmVEGF-null hearts despite a significant reduction of endothelial cell number. This finding is consistent with increased expression of Flt-1 and Tie-2 on individual endothelial cells and can be construed as further evidence of hypoxic induction in the cmVEGF-null hearts, as can the increase noted in erythropoietin expression. Assuming that the cardiac dysfunction in cmVEGF-null mice is ischemia related, the mechanism of ischemic dysfunction must be considered. Severe prolonged myocardial ischemia leads to cardiomyocyte necrosis with cardiac dysfunction on the basis of reduced myocardial mass. Chronic recurrent ischemia of a milder degree can lead to contractile dysfunction without myocyte necrosis—a phenomenon that can be caused by prolonged "stunning" or the development of "hibernating myocardium" (25, 26). cmVEGF-null hearts do not exhibit evidence of necrosis or replacement fibrosis. The observed left ventricular pump dysfunction in these hearts may thus be a form of myocardial stunning or hibernation, similar to that seen in some patients with advanced coronary artery disease (12, 25). In this scenario, adaptive molecular events that make the cardiomyocyte less susceptible to ischemia also lead to reduced contractile function, although the molecular alterations associated with chronic recurrent cardiac ischemia are characterized poorly. cmVEGF-null mice represent a viable murine model of myocardial contractile dysfunction associated with hypovascularity and induction of ischemic markers in the absence of myocardial necrosis. Thus, these mice may prove a valuable model system for studying the molecular events associated with chronic myocardial ischemia.

cmVEGF-null hearts demonstrate a blunted contractile response to increasing levels of β-adrenergic stimulation. The mechanism of this response is unclear, and may reflect either impaired β-adrenergic responsiveness or a reduced contractile reserve. Alterations in the β-adrenergic receptor–adenylate cyclase system have been documented during myocardial ischemia/hypoxia, and it is possible that ischemia in cmVEGF-null hearts has altered dobutamine responsiveness by such mechanisms (27). Conversely, the blunted dobutamine response may be caused by myocardial ischemia in the hypovascular cmVEGF-null hearts at the higher workloads induced by β-adrenergic stimulation. cmVEGF-null hearts do exhibit an increase in ejection fraction with dobutamine despite the blunted response in contractility. This response may be explained by the vasodilating effects of dobutamine on the peripheral vasculature resulting in a significant reduction in cardiac afterload.

The possibility also should be considered that the contractile dysfunction of these cmVEGF-null adult hearts is an inevitable consequence of abnormal embryonic cardiac development and postnatal cardiac growth (28). These thin-walled and dilated hearts may be at a mechanical disadvantage based primarily on their morphology, irrespective of an active ischemic process. Further, on the basis of the LaPlace relationship, a thin-walled dilated cardiac morphology can increase ventricular wall stress and myocardial oxygen demand, thus potentiating any tendency toward ischemia resulting from hypovascularization (29). In this manner, early cardiac development may define adult heart function.

In addition to the induction of hypoxia-inducible genes noted above, gene-expression profiling by real-time RT-PCR revealed several interesting findings and trends that provide insight into the coordinated expression of cytokines and receptors in the heart. The absence of a compensatory increase in VEGFs B and C, and indeed a significant decrease in VEGF family member placental growth factor in the cmVEGF-null hearts despite hypovascularity and cardiac dysfunction, suggests that control of these genes is complex. The increase in angiopoietin (Ang)-3 expression is also interesting and may relate to findings that Ang-3 expression is down-regulated in response to VEGF (30). Transforming growth factor β has been reported to be hypoxia/ischemia responsive, a possible explanation for the increase in

this gene in the cmVEGF-null hearts (31). Reductions in Tie-1, Flk-1, and Flt-4 expression likely reflect the decrease in endothelial cells in cmVEGF-null hearts. The decrease in Flk-1 expression may also reflect loss of positive up-regulation by VEGF (32).

The cmVEGF-null phenotype is less severe than that of the global VEGF deletion. Global heterozygous and homozygous VEGF KO embryos die during midgestation (≈E9.5–E10.5) and have extensive cardiovascular defects (18, 33). The dorsal aortae are diminished markedly or are absent, and heart development is abnormal with lack of cardiomyoblast differentiation. Conversely, the aorta and coronary macrovasculature are normal in the cmVEGF-null mice, and apart from a reduced number of microvessels, we observed no significant histologic abnormalities in the myocardium at E13.5 or adulthood. Further, the heterozygotes seem entirely normal. One explanation is that secretion of VEGF by nonmyocytes in the cardiac anlage can partially rescue cardiac development. Another is that failure of normal cardiac development in the global KO is secondary to other developmental defects that are not present in the cmVEGF-null mice, such as abnormal development of the aorta.

The general aim of this study was to investigate the role of cardiomyocytes as mediators of paracrine signaling in the heart. The specific focus was delineation of the role of cardiomyocyte-derived VEGF in coronary vascular development and in determination of adult heart function. Previous studies of nonconditional global VEGF or VEGF isoform gene deletions have demonstrated embryonic and early postnatal mortality associated with severe cardiac abnormalities and abnormal vascularization of other organs; thus establishing that systemic VEGF expression is essential and that VEGF isoform function is not equivalent (18, 33, 34). These systemic KO approaches do not address the specific role of VEGF expression in the heart or the relative importance of the cardiac myocyte in the secretion of this molecule. Furthermore, it is unclear whether cardiac abnormalities noted in these studies are primary or secondary to systemic developmental effects of global VEGF gene deletion. Conversely, the data presented here provide definitive evidence of the critical importance of cardiomyocyte-derived VEGF, establish an essential role for the cardiac myocyte as a secretory cell, and demonstrate that a cardiac-specific genetic alteration can have systemic effects—as exemplified by the lower body weights of the cmVEGF mice. Further, we have established a viable mouse model of cardiac hypovascularity with contractile dysfunction and evidence of ischemia. This model may prove useful to study the effects of angiogenic growth factors in the heart, and to study the molecular mechanisms associated with ischemic contractile dysfunction. Similar conditional gene-targeting approaches may also facilitate further study of paracrine pathways and myocyte to nonmyocyte communication in the heart.

We thank Hope Steinmetz and John Haeffel for PECAM antibody-binding experiments, Ben Shen for RNA isolation, and Mabel Chu for assistance in genotyping. We also thank Monique LaCorbiere for administrative support and Julie Sheridan for maintenance of transgenic colonies. This work was supported by the American Heart Association Grant 9730083N (to F.J.G.).

1. Long, C. S., Henrich, C. J. & Simpson, P. C. (1991) *Cell Regul.* **2**, 1081–1095.
2. Shah, A. M., Grocott-Mason, R. M., Pepper, C. B., Mebazaa, A., Henderson, A. H., Lewis, M. J. & Paulus, W. J. (1996) *Prog. Cardiovasc. Dis.* **39**, 263–284.
3. Gray, M. O., Long, C. S., Kalinyak, J. E., Li, H. T. & Karliner, J. S. (1998) *Cardiovasc. Res.* **40**, 352–363.
4. Hirota, H., Chen, J., Betz, U. A. K., Rajewsky, K., Gu, Y., Ross, J., Jr., Muller, W. & Chien, K. R. (1999) *Cell* **97**, 189–198.
5. Zak, R. (1973) *Am. J. Cardiol.* **31**, 211–219.
6. Nag, A. C. (1980) *Cytobios* **28**, 41–61.
7. Takahashi, N., Calderone, A., Izzo, N. J., Jr., Maki, T. M., Marsh, J. D. & Colucci, W. S. (1994) *J. Clin. Invest.* **94**, 1470–1476.
8. Coker, M. L., Doscher, M. A., Thomas, C. V., Galis, Z. S. & Spinale, F. G. (1999) *Am. J. Physiol.* **277**, H777–H787.
9. Bryant, D., Becker, L., Richardson, J., Shelton, J., Franco, F., Peshock, R., Thompson, M. & Giroir, B. (1998) *Circulation* **97**, 1375–1381.
10. Gerber, H. P., Hillan, K. J., Ryan, A. M., Kowalski, J., Keller, G. A., Rangell, L., Wright, B. D., Radtke, F., Aguet, M. & Ferrara, N. (1999) *Development (Cambridge, U.K.)* **126**, 1149–1159.
11. Rajewsky, K., Gu, H., Kuhn, R., Betz, U. A., Muller, W., Roes, J. & Schwenk, F. (1996) *J. Clin. Invest.* **98**, 600–603.
12. Heusch, G. (1998) *Physiol. Rev.* **78**, 1055–1085.
13. Minamisawa, S., Gu, Y, Ross, J., Jr., Chien, K. R. & Chen, J. (1999) *J. Biol. Chem.* **274**, 10066–10070.
14. Tanaka, N., Dalton, N., Mao, L., Rockman, H. A., Peterson, K. L., Gottshall, K. R., Hunter, J. J., Chien, K. R. & Ross, J., Jr. (1996) *Circulation* **94**, 1109–1117.
15. He, H., Giordano, F. J., Hilal-Dandan, R., Choi, D. J., Rockman, H. A., McDonough, P. M., Bluhm, W. F., Meyer, M., Sayen, M. R., Swanson, E. & Dillmann, W. H. (1997) *J. Clin. Invest.* **100**, 380–389.
16. Gibson, U. E., Heid, C. A. & Williams, P. M. (1996) *Genome Res.* **6**, 995–1001.
17. Eppihimer, M. J., Russell, J., Langley, R., Vallien, G., Anderson, D. C. & Granger, D. N. (1998) *Microcirculation* **5**, 179–188.
18. Ferrara, N., Carver-Moore, K., Chen, H., Dowd, M. L., O'Shea, K. S., Powell-Braxton, L., Hillan, K. J. & Moore, M. W. (1996) *Nature (London)* **380**, 439–442.
19. Ryan, H. E., Lo, J. & Johnson, R. S. (1998) *EMBO J.* **17**, 3005–3015.
20. Iyer, N. V., Kotch, L. E., Agani, F., Leung, S. W., Laughner, E., Wenger, R. H., Gassmann, M., Gearhart, J. D., Lawler, A. M., Yu, A. Y. & Semenza, G. L. (1998) *Genes Dev.* **12**, 149–162.
21. Li, J., Brown, L. F., Hibberd, M. G., Grossman, J. D., Morgan, J.P. & Simons, M. (1996) *Am. J. Physiol.* **270**, H1803–H1811.
22. Giordano, F. J., Ping, P., McKirnan, M. D., Nozaki, S., DeMaria, A. N., Dillmann, W. H., Mathieu-Costello, O. & Hammond, H. K. (1996) *Nat. Med.* **2**, 534–539.
23. Hendel, R. C., Henry, T. D., Rocha-Singh, K., Isner, J. M., Kereiakes, D. J., Giordano, F. J., Simons, M. & Bonow, R. O. (2000) *Circulation* **101**, 118–121.
24. Laham, R. J., Sellke, F. W., Edelman, E. R., Pearlman, J. D., Ware, J. A., Brown, D. L., Gold, J. P. & Simons, M. (1999) *Circulation* **100**, 1865–1871.
25. Kloner, R. A., Bolli, R., Marban, E., Reinlib, L. & Braunwald, E. (1998) *Circulation* **97**, 1848–1867.
26. Canty, J. M. & Fallavollita, J. A. (1999) *Am. J. Physiol.* **46**, H417–H422.
27. Kacimi, R., Richalet, J.-P., Corsin, A., Abousahl, I. & Crozatier, B. (1992) *J. Appl. Physiol.* **73**, 1377–1382.
28. Hudlicka, O. & Brown, M. D. (1996) *J. Vasc. Res.* **33**, 266–287.
29. Parmley, W. W. (1985) *Am. J. Cardiol.* **56**, 7A–11A.
30. Nishimura, M., Miki, T., Yashima, R., Yokoi, N., Yano, H., Sato, Y. & Seino, S. (1999) *FEBS Lett.* **448**, 254–256.
31. Falanga, V., Qian, S. W., Danielpour, D., Katz, M. H., Roberts, A. B. & Sporn, M. B. (1991) *J. Invest. Dermatol.* **97**, 634–637.
32. Shen, B. Q., Lee, D. Y., Gerber, H. P., Keyt, B. A., Ferrara, N. & Zioncheck, T. F. (1998) *J. Biol. Chem.* **273**, 29979–29985.
33. Carmeliet, P., Ferreira, V., Breier, G., Pollefeyt, S., Kieckens, L., Gertsenstein, M., Fahrig, M., Vandenhoeck, A., Harpal, K., Eberhardt, C., *et al.* (1996) *Nature (London)* **380**, 435–439.
34. Carmeliet, P., Ng, Y. S., Nuyens, D., Theilmeier, G., Brusselmans, K., Cornelissen, I., Ehler, E., Kakkar, V. V., Stalmans, I., Mattot, V., *et al.* (1999) *Nat. Med.* **5**, 495–502.